ISSN 1674-1056
http://cpb.iphy.ac.cn
http://iopscience.iop.org/cpb
中国物理 B
Chinese Physics
中国物理 Chinese Physics B

Critical behavior and magnetocaloric effect in magnetic Weyl semimetal candidate $Co_{2-x}ZrSn$

Tianlin Yu(于天麟), Xiaoyun Yu(余骁昀), En Yang(杨恩), Chang Sun(孙畅), Xiao Zhang(张晓), Ming Lei(雷鸣)

Citation: Chin. Phys. B . 2019, 28(6): 067501. **doi:** 10.1088/1674-1056/28/6/067501
Journal homepage: http://cpb.iphy.ac.cn; http://iopscience.iop.org/cpb

What follows is a list of articles you may be interested in

Magnetic properties and magnetocaloric effects in $(Ho_{1-x}Y_x)_5Pd_2$ compounds

X F Wu(武小飞), C P Guo(郭翠萍), G Cheng(成钢), C R Li(李长荣), J Wang(王江), Y S Du(杜玉松), G H Rao(饶光辉), Z M Du(杜振民)

Chin. Phys. B . 2019, 28(5): 057502. **doi:** 10.1088/1674-1056/28/5/057502

Ferromagnetism and magnetostructural coupling in V-doped MnNiGe alloys

Hui Yang(杨慧), Jun Liu(刘俊), Chao Li(李超), Guang-Long Wang(王广龙), Yuan-Yuan Gong(龚元元), Feng Xu(徐锋)

Chin. Phys. B . 2018, 27(10): 107502. **doi:** 10.1088/1674-1056/27/10/107502

Magnetostructural transformation and magnetocaloric effect in $Mn_{48-x}V_xNi_{42}Sn_{10}$ ferromagnetic shape memory alloys

Najam ul Hassan, Ishfaq Ahmad Shah, Tahira Khan, Jun Liu(刘俊), Yuanyuan Gong(龚元元), Xuefei Miao(缪雪飞), Feng Xu(徐锋)

Chin. Phys. B . 2018, 27(3): 037504. **doi:** 10.1088/1674-1056/27/3/037504

Magnetocaloric effect in the layered organic-inorganic hybrid $(CH_3NH_3)_2CuCl_4$

Yinina Ma(马怡妮娜), Kun Zhai(翟昆), Liqin Yan(闫丽琴), Yisheng Chai(柴一晟), Dashan Shang(尚大山), Young Sun(孙阳)

Chin. Phys. B . 2018, 27(2): 027501. **doi:** 10.1088/1674-1056/27/2/027501

Influences of La and Ce doping on giant magnetocaloric effect of EuTiO

Zhao-Jun Mo(莫兆军), Qi-Lei Sun(孙启磊), Jun Shen(沈俊), Mo Yang(杨墨), Yu-Jin Li(黎玉进), Lan Li(李岚), Guo-Dong Liu(刘国栋), Cheng-Chun Tang(唐成春), Fan-Bin Meng(孟凡斌)

Chin. Phys. B . 2018, 27(1): 017501. **doi:** 10.1088/1674-1056/27/1/017501

Critical behavior and magnetocaloric effect in magnetic Weyl semimetal candidate $Co_{2-x}ZrSn$*

Tianlin Yu(于天麟), Xiaoyun Yu(余骁昀), En Yang(杨恩), Chang Sun(孙畅), Xiao Zhang(张晓)†, and Ming Lei(雷鸣)‡

State Key Laboratory of Information Photonics and Optical Communications & School of Science, Beijing University of Posts and Telecommunications, Beijing 100876, *China*

(Received 22 February 2019; revised manuscript received 29 March 2019; published online 8 May 2019)

We investigate the critical exponents and magnetocaloric effect of $Co_{2-x}ZrSn$ polycrystal. The $Co_{2-x}ZrSn$ undergoes a second-order ferromagnetism phase transition around the Curie temperature of $T_c \sim 280$ K. The critical behavior in the vicinity of the magnetic phase transition has been investigated by using modified Arrott plot and Kouvel–Fisher methods. The obtained critical exponents, β, γ, and δ can be well described by the scaling theory. The determined exponents of $Co_{2-x}ZrSn$ obey the mean-field model with a long-range magnetic interaction. In addition, the maximum magnetic entropy change $-\Delta S_M^{max}$ of $Co_{2-x}ZrSn$ is about 0.57 J·kg^{-1}·K^{-1} and the relative cooling power (RCP) is 14.68 J·kg^{-1} at 50 kOe (1 Oe = 79.5775 A·m^{-1}).

Keywords: critical phenomena, magnetocaloric effect, Heusler compound

PACS: 75.40.Cx, 75.20.En, 75.30.Sg, 75.50.Cc **DOI:** 10.1088/1674-1056/28/6/067501

1. Introduction

In the last decade, intensive research of the topology of electronic structures has deepened our understanding of the exotic physical properties of novel condensed matters and established a whole new classification. After the discovery of topological insulators,[1,2] topological semimetals (TSMs) have attracted considerable attention in recent years. The TSMs are characterized by the symmetry protected bulk band crossings near the Fermi energy E_F.[3–6] According to the degeneracy of nodes, they can be classified into Dirac semimetals (DSMs), Weyl semimetals (WSMs), multi-degenerate semimetals, and so on.[7] Among these TSMs, DSMs have Dirac nodes that can be viewed as two Weyl nodes with opposite chirality degenerate at the same k-point. Such a degeneracy can be lifted by breaking either inversion symmetry (IS) or time-reversal symmetry (TRS), resulting in two types of WSMs; *i.e.*, nonmagnetic noncentrosymmetric WSMs and magnetic WSMs.[7] The first class of WSMs has been theoretically predicted and experimentally confirmed.[8–10] Magnetic WSMs have been predicted in several materials, such as pyrochlore iridates, Heusler compounds, and the related materials such as Heusler alloys Co_2TiX (X = Si, Ge, or Sn), Co_2MnAl, and half-Heusler compound GdPtBi, *etc*.[4,11–14]

Recently, Heusler compound Co_2ZrSn has also been predicted to host Weyl fermions.[15] Moreover, it belongs to the family of 26 valence electron Heusler systems, which are known to exhibit half-metallic ferromagnetism (HMFM) with saturated magnetic moments of $\sim 2\ \mu_B$ per formula unit.[16,17] According to the classification proposed by Coey,[18] Co_2ZrSn is a type of I_A HMFM, in which the spin-majority band is crossing E_F (metallic) and there is a band gap for the spin-minority band. Because it is an HMFM compound with Curie temperature (T_c) near/higher than room temperature,[19] besides the unique feature of harboring Weyl fermions, it is vitally important to the spintronics applications due to the nearly 100% spin polarization of conduction electrons at E_F.[20] Previous studies on Co_2ZrSn single crystals show that there are some vacancies in the position of Co with the content of Co varying from 1.59 to 1.84. With higher Co content, the sample exhibits higher T_c and the T_c is above room temperature when the content of Co is larger than 1.70.[19] Meanwhile, when Cu is doped into the Co site, the T_c of $Co_{2-y}Cu_xZrSn$ decreases linearly and the low-temperature spin glass behavior appears when y is close to 1.[21] This trend can be explained by the weakening of half-metallicity of Co_2ZrSn with the Cu substitutions, leading to the breakdown of the ferromagnetism.[21] To understand the itinerant ferromagnetism in Co_2ZrSn further, a comprehensive investigation of phase transition and critical exponents is urgently needed, which will not only provide an insight into the range of ferromagnetic interaction but also the symmetry of the order parameter within a given universality class.[22,23] Among the various properties of ferromagnets, magnetocaloric effect (MCE) is another important feature that can be used for magnetic refrigeration, which is an environmentally friendly energy-conversion technology.

In this paper, the magnetic critical behavior and mag-

*Project supported by the Fundamental Research Funds for the Central Universities (Grant No. 2017RC20) and the Research Innovation Fund for College Students of Beijing University of Posts and Telecommunications.

†Corresponding author. E-mail: zhangxiaobupt@bupt.edu.cn

‡Corresponding author. E-mail: mlei@bupt.edu.cn

© 2019 Chinese Physical Society and IOP Publishing Ltd

netocaloric effect of $Co_{2-x}ZrSn$ in the vicinity of the paramagnetic–ferromagnetic (PM–FM) phase transition region are studied in detail. It is found that $Co_{2-x}ZrSn$ undergoes a second-order phase transition with a long-range order in the nature of magnetic interaction. Moreover, the obtained critical exponents are found to follow the theoretically predicted values for mean-field model. Further analysis of the field-dependent magnetic entropy change $-\Delta S_M(T,H)$ indicates that the maximum magnetic entropy change $-\Delta S_M^{max}$ of $Co_{2-x}ZrSn$ is about 0.57 J·kg^{-1}·K^{-1} at 50 kOe.

2. Experimental

Polycrystal $Co_{2-x}ZrSn$ was synthesized using arc-melting method under an Ar atmosphere. High purity Zr particles and Co pieces were melted first to achieve a homogeneous mixture of the compound metal. Then, the obtained alloy was brought close to the Sn shots and remelted. The sample was flipped three times to avoid breaking up over a long time of arc-melting. Finally the arc-melted sample was cooling down naturally. The crystal structure and phase purity were identified by powder x-ray diffraction (pXRD) using the Cu–Kα radiation of Bruker D8. Rietveld refinements of the data were performed with the TOPAS package.[24] The magnetization measurements were conducted using a Quantum Design MPMS3.

3. Results and discussion

The XRD patterns of $Co_{2-x}ZrSn$ can be readily indexed to the crystal structures of Heusler L21 phase ($Fm3m$) (Fig. 1(a)). No obvious characteristic peaks of other impurities are detected. The intense diffraction peaks suggest that the as-synthesized products are well crystallized. The fitted lattice parameter a is 6.21266(8) Å. When compared to previous single crystal results, it suggests that the value of x in $Co_{2-x}ZrSn$ is about 0.33.[19] The temperature dependence of magnetization $M(T)$ at $H = 1$ kOe with zero-field-cooling (ZFC) and field-cooling (FC) models are plotted in Fig. 1(b). The $M(T)$ curves show a typical PM–FM phase transition. Inset of Fig. 1(b) shows the T_c is ~ 280 K, which is defined as the minimum value of the $dM(T)/dT$. This is consistent with previous results for $Co_{2-x}ZrSn$ single crystals.[19] The overlap of ZFC and FC $M(T)$ curves suggests the absence of spin-glass behavior in $Co_{2-x}ZrSn$. Figure 1(c) shows the magnetization hysteresis loop of $Co_{2-x}ZrSn$ measured at 2 K. The saturated moment M_s is about 1 μ_B/f.u., in agreement with that of $Co_{2-x}ZrSn$ single crystals.[19] Meanwhile, the magnetic coercivity (H_c) of $Co_{2-x}ZrSn$ is smaller than 50 Oe, which indicates the $Co_{2-x}ZrSn$ is a super soft magnet.

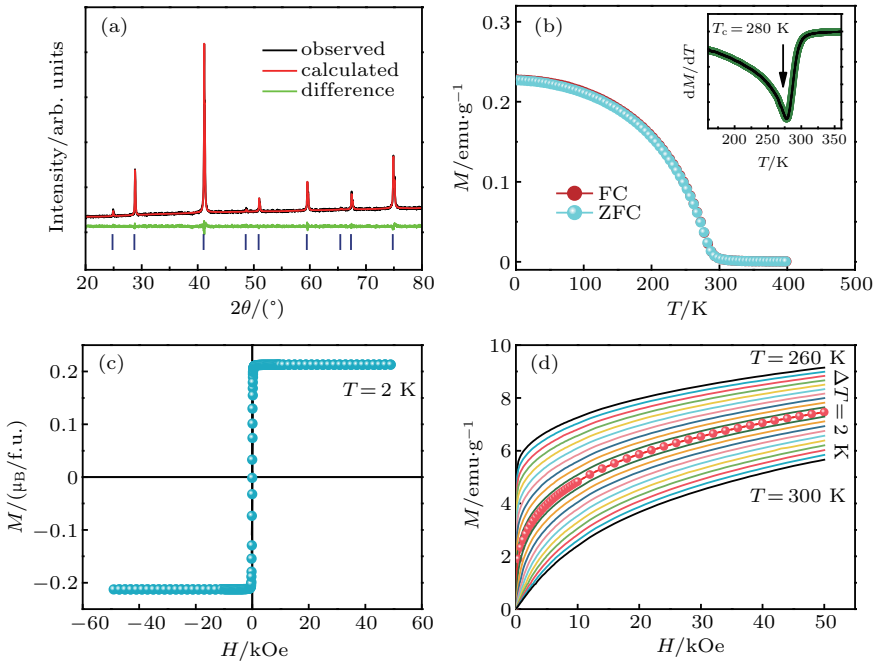


Fig. 1. (a) The powder XRD pattern and Rietveld refinement of $Co_{2-x}ZrSn$. Vertical tick marks is Bragg reflections in the $Fm3m$ space group. (b) Temperature dependence of magnetization at $H = 1$ kOe with ZFC and FC modes. Inset: $dM(T)/dT$ as a function of temperature near T_c. (c) Isothermal $M(H)$ loop at 2 K. (d) Isothermal magnetization curves from 260 K to 300 K with 2-K temperature interval.

To further understand the fundamental feature of the FM phase transition in $Co_{2-x}ZrSn$, we measured the isothermal magnetization curves $M(H)$ from 260 K to 300 K with temperature step of 2 K as shown in Fig. 1(d). According to the mean-field theory, the ferromagnet undergoes a second order phase transition with long range order interactions, the Landau free energy $G(T,M)$ could be expressed as:[25]

$$G(T,M) \cong G_0 + \frac{1}{2}A(T)M^2 + \frac{1}{4}B(T)M^4 + \cdots - M(\mu_0 H), \quad (1)$$

where A and B are temperature-dependent parameters. When the free energy $G(T,M)$ is minimal, $(\partial G/\partial M) = 0$, the equation of state can be expressed as:

$$H/M = A + BM^2. \tag{2}$$

Based on this equation, we can plot a Arrott plot of M^2 *versus* H/M, which should be a series of straight lines, and the positive intercepts of these straight lines on the H/M axis determine the second-order magnetic transition. But we should analyze the $M(H)$ results for the short-range FM phase transition systems by using the Arrot–Noaks equation of state $(H/M)^{1/\gamma} = a\varepsilon + bM^{1/\beta}$, where $\varepsilon = (T - T_c)/T_c$ is the reduced temperature, and a and b are constants.[26] We constructed the Arrott plots, using 3D XY model ($\beta = 0.345$, $\gamma = 1.316$), 3D Heisenberg model ($\beta = 0.365$, $\gamma = 1.386$), 3D Ising model ($\beta = 0.325$, $\gamma = 1.24$), and mean field model ($\beta = 0.5$, $\gamma = 1.0$), as given in Fig. 2. All these models yield quasi-straight lines in the high-field region, the positive intercepts reveals a second-order PM–FM transition in $Co_{2-x}ZrSn$. However, none of the models yield a series of parallel straight lines in the high-field range and the line at T_c passes through the origin. Therefore, it is difficult to distinguish which model is the best for the determination of critical exponents.

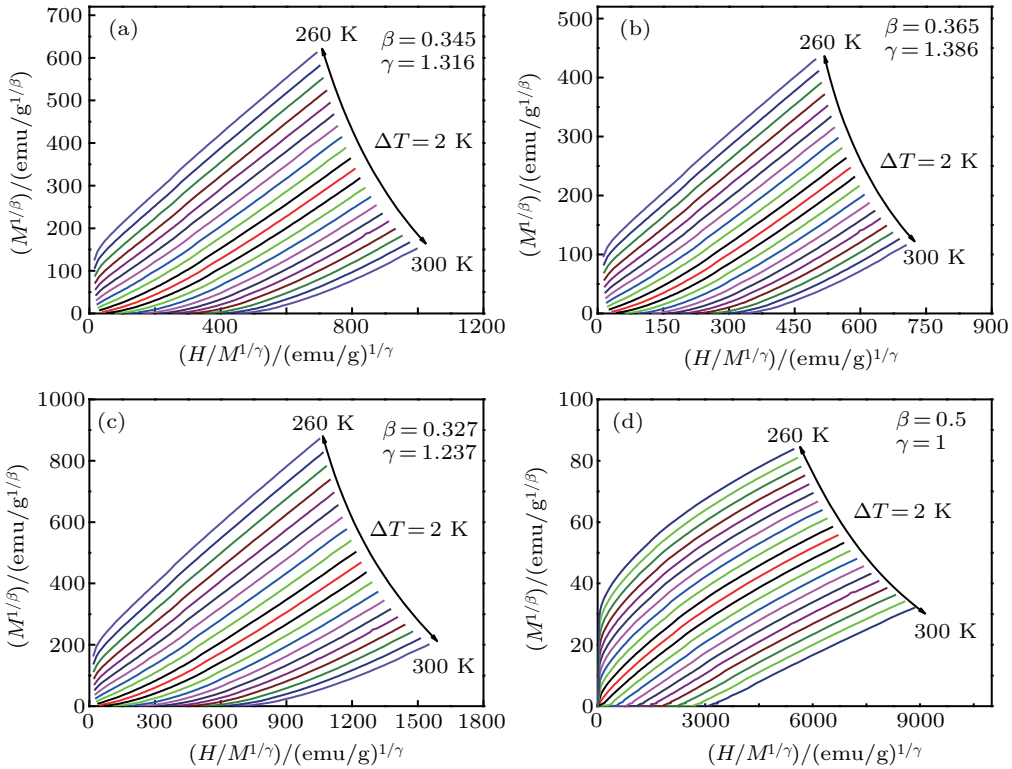


Fig. 2. The MAP of (a) 3D XY model, (b) 3D Heisenberg model, (c) 3D Ising model, and (d) mean-field model.

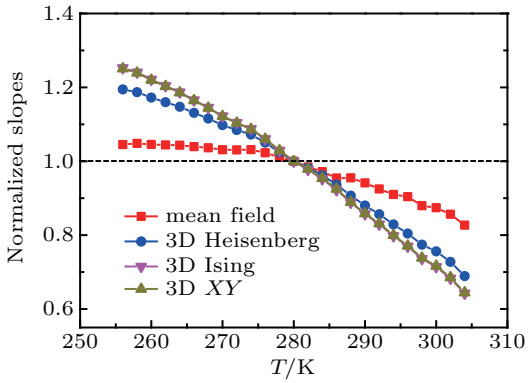


Fig. 3. Temperature dependence of the normalized slopes NS = $S(T)/S(T_c)$.

To determine better parameters, we calculated their normalized slopes (NS) which are defined at the critical point as NS = $S(T)/S(T_c)$, where $S(T)$ is the slope of $M^{1/\beta}$ *versus* $(H/M)^{1/\gamma}$ at high field. Because the most appropriate model should be the one close to 1.0 in the vicinity of T_c,[27] the mean-field is the best model for $Co_{2-x}ZrSn$ system, as shown in Fig. 3. However, the Arrott plot with the critical exponents $\beta = 0.5$ and $\gamma = 1$ could not lead to a set of parallel lines in the high magnetic field region. According to the scaling hypothesis, critical exponents β and γ can be briefly described by the following equation,[25,28]

$$M_s(T) = M_0(-\varepsilon)^{\beta}, \quad \varepsilon < 0, \quad T < T_c, \tag{3}$$

$$\chi_0^{-1}(T) = (h_0/M_0)\varepsilon^{\gamma}, \quad \varepsilon > 0, \quad T > T_c, \tag{4}$$

$$M = DH^{1/\delta}, \quad \varepsilon = 0, \quad T = T_c, \tag{5}$$

where $M_s(T)$ is the spontaneous magnetization below T_c, $\chi_0^{-1}(T)$ the inverse initial susceptibility $\chi_0^{-1}(T)$ above T_c, $\varepsilon = (T - T_c)/T_c$ is the reduced temperature and M_0, h_0/m_0,

and D are the critical amplitudes. Starting from the initial trial values of $\beta = 0.5$ and $\gamma = 1$, $M_s(T)$ and $\chi_0^{-1}(T)$ obtained from the linear extrapolation are then fitted to Eqs. (2) and (4), respectively, yielding new values of β, γ and T_c. Repeat the iterative process until β and γ are stable. The final modified Arrott plot (MAP) generates the values $\beta = 0.41(1)$ and $\gamma = 1.08(9)$, and two sets of $M_s(T)$ and $\chi_0^{-1}(T)$ with the fitting curves are shown in Fig. 4(a). The fixed T_c values from two curves are consistent with each other (280.1(8) K and 280.3(7) K). Thus, the T_c of $Co_{2-x}ZrSn$ is 280 K, which is consistent with the values obtained from the $M(T)$ curve. A further possibility to evaluate the values of β, γ, and T_c is given by the Kouvel–Fisher (KF) method,[29]

$$M_s(T)/(\mathrm{d}M_s(T)/\mathrm{d}T) = (T - T_c)/\beta, \tag{6}$$

$$\chi_0^{-1}(T)/(\mathrm{d}\chi_0^{-1}(T)/\mathrm{d}T) = (T - T_c)/\gamma. \tag{7}$$

Figure 4(b) shows that the critical exponents obtained from the KF method are $\beta = 0.415(2)$ with $T_c = 280.1(7)$ K and $\gamma = 1.08(5)$ with $T_c = 280.4(1)$ K. These are consistent with the values derived from the modified Arrott plots. The critical exponent δ can be determined by the critical isotherm analysis from $M(H)$ at T_c following Eq. (5). The isothermal magnetization $M(H)$ at $T_c = 280$ K is shown in Fig 4(c), where the inset plots with the logarithmic scale. The inset shows that the $\log(M)$–$\log(H)$ relation yields straight line at higher field range with the slope $1/\delta$, where $\delta = 3.53$ is obtained. According to the statistical theory, the critical exponents should agree with the Widom scaling relation:[30]

$$\delta = 1 + \gamma/\beta. \tag{8}$$

Using the β and γ values determined from the modified Arrott plot and Kouvel–Fisher (KF) plot, we obtain $\delta = 3.66$ and $\delta = 3.61$, respectively, which close to the above value of δ. Furthermore, there is an important criterion for the critical regime based on the prediction of scaling hypothesis,[25]

$$M(H, \varepsilon) = \varepsilon^{\beta} f \pm (H/\varepsilon^{\beta+\gamma}), \tag{9}$$

where f_+ is used for $T > T_c$ and f_- is used for $T < T_c$. Then, the precise value of β and γ are used in fitting the plot of Fig. 4(d). the $M|\varepsilon|^{-\beta}$ as a function of $H|\varepsilon|^{-(\beta+\gamma)}$ plots in the critical region should collapse into two universal curves: one above T_c and another below T_c. The emergence of two convergence curves in Fig. 4(d) indicate the critical exponents are correct and reliable.

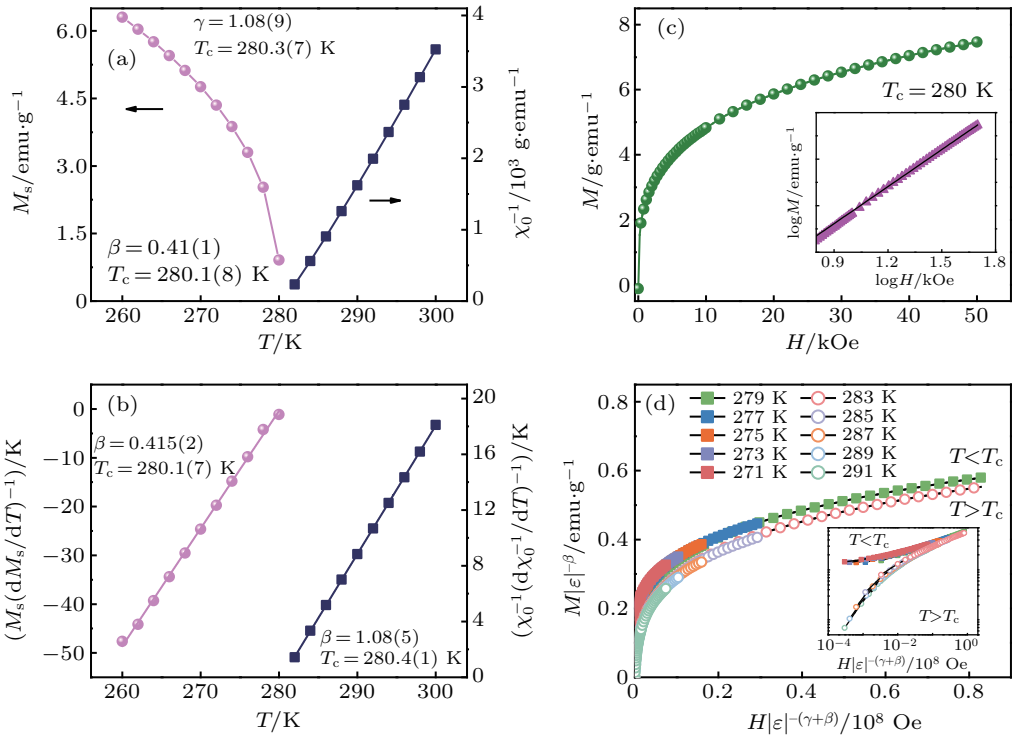


Fig. 4. (a) The MAP plot for M_s *versus* T (left) and χ_0^{-1} *versus* T (right). (b) The KF plot for $M_s(T)(\mathrm{d}M_s(T)/\mathrm{d}T)^{-1}$ *versus* T (left) and $\chi_0^{-1}(T)(\mathrm{d}\chi_0^{-1}(T)/\mathrm{d}T)^{-1}$ *versus* T. (c) The plot of the isotherm M *versus* H around $T = 280$ K. Insert: $\log(M)$ *versus* $\log(H)$. (d) Scaling plots of M *versus* H below and above $T_c = 280$ K. Isert: $\log(M)$ *versus* $\log(H)$.

The universality class of the magnetic phase transition depends on range of the exchange distance $J(r)$. It decays as $J(r) \sim r^{-(d+\sigma)}$, where σ is the range of the interaction, r is the distance, d is the dimensionality, and b is the spatial scaling factor. The the parameter of σ can be calculated by the equation,[31]

$$\gamma = 1 + \frac{4}{d}\frac{n+2}{n+8}\Delta\sigma + \frac{8(n+2)(n-4)}{d^2(n+8)^2}$$

$$\times\left[1+\frac{2G(\frac{d}{2})(7n+20)}{(n-4)(n+8)}\right]\Delta\sigma^2, \tag{10}$$

where n is the spin dimensionality, $\Delta\sigma=\sigma-d/2$, $G(d/2)=3-\frac{1}{4}(d/2)^2$. According to the renormalization group analysis, the spin interactions can be classified by the value of σ. The $\sigma<2$ implies long-range spin interaction dominated in the system, while $\sigma>2$ implies the short-range spin interaction. In the $Co_{2-x}ZrSn$ system, the experimental value of γ is 1.26, for any combination of $\{d:n\}$ the values of σ are always smaller than 2. This suggests that the long-range spin interaction plays an important role in the $Co_{2-x}ZrSn$ system.

To gain more information on critical properties of $Co_{2-x}ZrSn$, we have studied the magnetic entropy change $-\Delta S_M(T,H)$. According to thermal dynamics, the magnetic entropy change $-\Delta S_M(T,H)$ is defined as,[32]

$$\begin{aligned}\Delta S_M(T,H) &= S_M(T,H)-S_M(T,0)\\ &= \int_0^H\left(\frac{\partial M}{\partial T}\right)_H \mathrm{d}H.\end{aligned} \tag{11}$$

For the magnetization measured at small discrete fields and temperature intervals, $-\Delta S_M(T,H)$ can be approximately expressed as,[33]

$$\left|\Delta S_M\left(\frac{T_i+T_{i+1}}{2}\right)\right|=\sum\left[\frac{(M_i-M_{i+1})_{H_i}}{T_{i+1}-T_i}\right]\Delta H_i, \tag{12}$$

where M_i and M_{i+1} are the magnetization at T_i and T_{i+1} under the same magnetic field, respectively. The calculated results for $\Delta S_M(T,H)$ have been shown in Fig. 5(a). It is obviously that the values of $-\Delta S_M$ at different magnetic fields reach the maximum in the vicinity of T_c. The maximum magnetic entropy change $-\Delta S_M^{max}$ is about 0.57 J·kg^{-1}·K^{-1} ($\sim$ 5.2 mJ·cm^{-3}·K^{-1}) for $H=50$ kOe. Figure 5(b) depicts the values of $-\Delta S_M^{max}$ vary with the magnetic fields. Generally, for the long-range spin interaction mean-filed model, $-\Delta S_M^{max}$ obeys the power law of $-\Delta S_M^{max}\propto H^{2/3}$. Fitting of the $-\Delta S_M^{max}$ gives that $n=0.696(3)$, confirming that the critical behavior of $Co_{2-x}ZrSn$ can be depicted by mean-field theory.

The relative cooling power (RCP) is also an important indicator for characterizing the magnetothermal material, its mathematical definition is,[34]

$$\mathrm{RCP}=-\Delta S_M^{max}\times\delta T_{FWHM}, \tag{13}$$

where the RCP is the function of T with $-\Delta S_M^{max}$ and the full width at half maximum δT_{FWHM}. The values of calculating the RCP at different fields are shown in Fig. 5(c). With the increasing of magnetic field, the RCP curve shows a linear trend. The RCP at $H=50$ kOe is about 14.68 J·kg^{-1} ($\sim$ 0.13 J·cm^{-3}). This value is smaller than those typical magnetocaloric materials[32] because of the relatively small $-\Delta S_M^{max}$. However, because the T_c of $Co_{2-x}ZrSn$ is close to or above room temperature, it would be interesting to develop a method that can improve the magnetocaloric property of $Co_{2-x}ZrSn$ in the future, such as the chemical doping method.

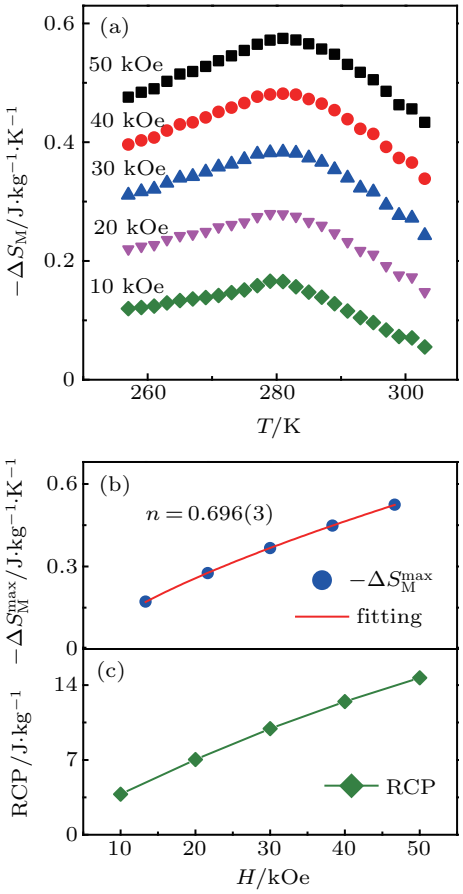


Fig. 5. (a) The trend plots of $-\Delta S_M$ with temperature variation at the different magnetic fields. (b) Field dependence of $-\Delta S_M^{max}$. The solid line represents a fit of H^n to the data. (c) Field dependence of RCP.

4. Conclusion

In summary, the magnetic properties of $Co_{2-x}ZrSn$ polycrystal are studied in detail. It is found that the PM–FM transition in $Co_{2-x}ZrSn$ polycrystal is the second-order phase transition. The critical exponents β, γ, and δ obtained from the MAP and KF methods are consistent each other. These parameters conform to the scaling rate very well. In addition, these critical exponents suggest that the magnetic transition of $Co_{2-x}ZrSn$ polycrystal can be described by the mean-field model. Moreover, the $-\Delta S_M^{max}$ and RCP are about 0.57 J·kg^{-1}·K^{-1} and 14.68 J·kg^{-1} at $H=50$ kOe, respectively.

References

[1] Hasan M Z and Kane C L 2010 *Rev. Mod. Phys.* **82** 3045
[2] Qi X L and Zhang S C 2011 *Rev. Mod. Phys.* **83** 1057
[3] Burkov A A, Hook M D and Balents L 2011 *Phys. Rev. B* **84** 235126
[4] Wan X, Turner A M, Vishwanath A and Savrasov S Y 2011 *Phys. Rev. B* **83** 205101
[5] Xu G, Weng H, Wang Z, Dai X and Fang Z 2011 *Phys. Rev. Lett.* **107** 186806
[6] Wang Z, Sun Y, Chen X Q, Franchini C, Xu G, Weng H, Dai X and Fang Z 2012 *Phys. Rev. B* **85** 195320
[7] Weng H M, Dai X and Fang Z 2016 *J. Phys.: Condens. Matter* **28** 303001
[8] Weng H M, Fang C, Fang Z, Bernevig B A and Dai X 2015 *Phys. Rev. X* **5** 011029

[9] Xu S Y, Belopolski I, Alidoust N, *et al.* 2015 *Science* **349** 613

[10] Lv B Q, Weng H M, Fu B B, Wang X P, Miao H, Ma J, Richard P, Huang X C, Zhao L X, Chen G F, Fang Z, Dai X, Qian T and Ding H 2015 *Phys. Rev. X* **5** 031013

[11] Chang G, Xu S Y, Zheng H, Singh B, Hsu C H, Bian G, Alidoust N, Belopolski I, Sanchez D S, Zhang S, Lin H and Hasan M Z 2016 *Sci. Rep.* **6** 38839

[12] Manna K, Sun Y, Muechler L, Kübler J and Felser C 2018 *Nat. Rev. Mat.* **3** 244

[13] Kübler J and Felser C 2016 *Europhys. Lett.* **114** 47005

[14] Hirschberger M, Kushwaha S, Wang Z, Gibson Q, Liang S, Belvin C A, Bernevig B A, Cava R J and Ong N P 2016 *Nat. Mater.* **15** 1161

[15] Wang Z, Vergniory M G, Kushwaha S, Hirschberger M, Chulkov E V, Ernst A, Ong N P, Cava R J and Bernevig B A 2016 *Phys. Rev. Lett.* **117** 236401

[16] Fecher G H, Kandpal H C, Wurmehl S, Felser C and Schönhense G 2006 *J. Appl. Phys.* **99** 08J106

[17] Kandpal H C, Fecher G H and Felser C 2007 *J. Phys. D: Appl. Phys.* **40** 1507

[18] Coey J M D, Venkatesan M 2002 *J. Appl. Phys.* **91** 8345

[19] Kushwaha S K, Stolze K, Wang Z, Hirschberger M, Lin J, Bernevig B A, Ong N P and Cava R J 2017 *J. Phys.: Condens. Matter* **29** 225702

[20] De Groot R A, Mueller F M, Engen P G and Buschow K H 1983 *Phys. Rev. Lett.* **50** 2024

[21] Kushwaha S K, Wang Z, Kong T and Cava R J 2018 *J. Phys.: Condens. Matter* **30** 075701

[22] Sondhi S L, Girvin S M, Carini J P and Shahar D 1997 *Rev. Mod. Phys.* **69** 315

[23] Banerjee B K 1964 *Phys. Lett.* **12** 16

[24] Bruker AXS. TOPAS Version 4.2 2009 *Bruker AXS*, Karlsruhe, Germany

[25] Stanley H E 1971 *Introduction to Phase transitions and critical phenomena* (London: Clarendon Press) p. 7

[26] Arrott A and Noakes J E 1967 *Phys. Rev. Lett.* **19** 786

[27] Fan J, Ling L, Hong B, Zhang L, Pi L and Zhang Y 2010 *Phys. Rev. B* **81** 144426

[28] Fisher M E 1967 *Rep. Prog. Phys.* **30** 615

[29] Kouvel J S and Fisher M E 1964 *Phys. Rev. A* **136** A1626

[30] Widom B 1965 *J. Chem. Phys.* **43** 3898

[31] Fischer S F, Kaul S N and Kronmuller H 2002 *Phys. Rev. B* **65** 064443

[32] Gschneidner Jr. K A, Pecharsky V K and Tsokol A O 2005 *Rep. Prog. Phys.* **68** 1479

[33] Phan M H and Yu S C 2007 *J. Magn. Magn. Mater.* **308** 325

[34] Han H, Menzel D, Liua W, Ling L, Dua H, Pi L, Zhanga C, Zhang L and Zhang Y 2017 *Mater. Res. Bull.* **94** 500